Trebst, C., Heine, S., Lienenklaus, S., Lindner, M., Baumgärtner, W., Weiss, S., Stangel, M.
Lack of interferon-beta leads to accelerated remyelination in a toxic model of central nervous system demyelination
(2007) Acta Neuropathologica, 114 (6), pp. 587-596.

Lack of Interferon-beta leads to accelerated remyelination in a toxic model of central nervous system demyelination

Corinna Trebst[1*] ,Sandra Heine[1*], Stefan Lienenklaus[3], Maren Lindner[1,2], Wolfgang Baumgärtner[2,4], Siegfried Weiss[3], Martin Stangel[1,2]

[1]Dept. of Neurology, Medical School Hannover, Hannover, Germany, [2]Center for Systems Neuroscience, Hannover, Germany and [3]Molecular Immunology Group, Helmholtz Center for Infection Research, Braunschweig, Germany, [4]Dept. of Pathology, Veterinary School Hannover, Germany

* These two authors contributed equally to this work.

Correspondence and reprint requests to:

Prof. Dr. Martin Stangel

Department of Neurology

Medical School Hannover

Carl-Neuberg-Str. 1

30625 Hannover

Germany

Phone: +49 511 532 6677

Fax: +49 511 532 3115

Email: stangel.martin@mh-hannover.de

Abstract

Interferon-beta (IFN-β) is a pleiotropic cytokine that is known to modulate the immune response in multiple sclerosis (MS), an inflammatory demyelinating disease of the central nervous system (CNS). Spontaneous remyelination and repair mechanisms in MS are mostly insufficient and contribute to clinical disability. Here, we investigated whether IFN-β has a potential in modifying the extent of de- and remyelination in a toxic model of CNS demyelination induced by the copper chelator cuprizone. IFN-β deficient (k/o) mice showed an accelerated spontaneous remyelination. However, the amount of remyelination after 6 weeks did not differ between the two groups. Demyelination in IFN-β k/o mice was paralleled by a diminished astrocytic and microglia response as compared to wildtype controls, whereas the accelerated remyelination was paralleled by an increased number of oligodendrocyte precursor cells (OPC) within the demyelinated lesion at the beginning of the remyelination phase. We hypothesize that the absence of IFN-β lead to more efficient recruitment and proliferation of OPC already during demyelination thus allowing early remyelination. These results demonstrate that IFN-β is able to alter remyelination in the absence of an immune-mediated demyelination.

Keywords: Interferon-beta; demyelination; remyelination; multiple sclerosis; cuprizone model

Introduction

Multiple sclerosis (MS) is generally considered a demyelinating disease of the central nervous system (CNS) mediated by an autoimmune reaction. It is well established that spontaneous remyelination is a consistent phenomenon in MS, occurring in about 50% of demyelinated plaques [17,24]. Remyelination can restore electrophysiologic functions and therefore also minimize long term disability [28]. Thus, enhancement of remyelination might be an effective mechanism to prevent secondary axonal damage [26]. To develop such a strategy a more detailed understanding of the molecular mechanisms of successful remyelination is required. This can be studied in animal models with toxic induced demyelination and subsequent spontaneous remyelination, such as the cuprizone model. Feeding of cuprizone (bis-cyclohexanone-oxaldihydrazone) to young adult mice induces a synchronous consistent, reproducible and complete demyelination of the corpus callosum and to a variable degree of the superior cerebellar peduncle within 6 weeks [19]. Removal of cuprizone from the diet leads to a spontaneous and almost complete remyelination. The cuprizone model is therefore an ideal animal model to study mechanisms of remyelination independent of a primary inflammatory insult or blood brain barrier injury.

It is commonly accepted that remyelination in the CNS is mediated by oligodendrocyte precursor cells (OPC) that proliferate, migrate and differentiate into mature oligodendrocytes producing myelin sheaths [33]. Factors which influence this process include growth factors, cytokines, chemokines, and hormones. Most of these factors are secreted by other glial cells (microglia and astrocytes) in the setting of demyelinated lesions [2]. Furthermore, glial-axon interactions are considered critical for successful remyelination [3].

Interferon-beta (IFN-β) represents a cytokine that is known to have a disease modifying effect in patients with relapsing-remitting MS. The exact mechanisms by which IFN-β modulates disease activity in MS are still not clear. Proposed mechanisms are regulation of expression of adhesion molecules and chemokines in the CNS, modulation of T cell and monocyte functions [4,32,5,7,31,11]. Furthermore, in vitro data showed that IFN-β influences glial cells such as microglia and astrocytes. For example, IFN-β downregulates the production of tumor necrosis factor-alpha by microglia [6] and upon stimulation by IFN-β astrocytes, produce interleukin 6 [23]. We have previously shown that IFN-β significantly inhibits the differentiation of OPC in vitro when cultured in the presence of microglia and astrocytes [10], suggesting that IFN-β may also influence remyelination. To investigate the role of IFN-β on remyelination in vivo, we used mice lacking IFN-β in the cuprizone model of MS.

Materials and Methods

Animals

The IFN-β k/o mice were originally developed with a neomycinR inserted targeting construct, transfected to the 129 strain ES cell E14, and backcrossed to the C57BL/6 background for more than 15 generations [8]. Mice were bred and kept in the animal facilities of the Helmholtz Center for Infection Research in Braunschweig, Germany. For wildtype (wt) controls C57BL/6 mice were purchased from Harlan (Netherlands). All experiments were performed according to the national animal laws and approved by the local government authority.

Developmental studies

Myelination as well as distribution and frequency of glial fibrillary acidic protein (GFAP)- and nerve/glial antigen 2 proteoglycan (NG2)-positive cells during development were studied in 1, 6, 21 day and 8 week old IFN-β k/o mice and wt controls in comparison. Animal perfusion and tissue processing was handled as described below.

Cuprizone model and tissue processing

8-week-old male IFN-β k/o and wt control mice were fed *ad libitum* 0.2% cuprizone (bis-cyclohexanone oxaldihydrazone, Sigma-Aldrich Inc., St.Louis, MO) mixed into a standard ground rodent chow. Cuprizone diet was maintained for 6 weeks (demyelination phase). After 6 weeks mice were put on a normal chow for another 6 weeks (remyelination phase). At each of 6 different time points (0, 3, 6, 7, 9 and 12 weeks) 5 IFN-β k/o and 5 wt animals were perfused with 4% paraformaldehyde (PFA)

in phosphate buffer via the left ventricle. Brains were removed and postfixed in 4% PFA. For immunohistochemical analyses brains were embedded in paraffin according to standard procedures. At the time points baseline, 6 weeks (complete demyelination) and 7 weeks (early remyelination) additionally 2-3 brains of IFN-β k/o and wt mice, respectively, were processed for electron microscopy (EM). Trimmed sections were postfixed in 2.5 % glutaraldehyde and further processed in 1% osmium tetroxide, dehydrated, and embedded in epon.

Immunohistochemistry and histology

Immunohistochemical (IHC) analysis was performed using an avidin-biotin-horseradish peroxidase complex procedure and 3,3-diaminobenzidine (DAB). In brief, 7 µm serial paraffin embedded sections at the level of section 220 to 300 according to the mouse atlas by Sidman were deparaffinized with xylenes and rehydrated in ethanol [27]. After antigen retrieval by microwaving in citrate buffer, slides were incubated overnight with primary antibody at 4°C, washed, incubated with secondary antibody at room temperature for 40 min, washed and incubated with avidin–biotin–horseradish peroxidase complex (Vectastain Elite, Vector Laboratories). After development with DAB substrate (Dako), slides were counterstained with hematoxylin, dehydrated with ethanol and mounted in Eukit (Kindler GmbH & Co, Germany). Primary antibodies were omitted in controls. The following antibodies were used: murine monoclonal anti-proteolipid protein (PLP, 1:500, Serotec), murine monoclonal anti-myelin basic protein (MBP, 1:1000, Sternberger Monoclonals Inc.), murine monoclonal anti-myelin oligodendrocyte glycoprotein (MOG, 1:5, hybridoma supernatant, generous gift by C. Linington), murine monoclonal anti-non-phosphorylated neurofilament (SMI 32, 1:1000, Sternberger Monoclonals Inc.), murine monoclonal anti-GFAP (1:200, Chemicon,

UK), rabbit polyclonal anti-NG2 (1:200, Chemicon, UK), rat monoclonal anti-MAC-3 (1:50, BD Pharmingen, Germany), rabbit anti-neurite outgrowth inhibitor protein A (Nogo-A, 1:750 Chemicon, UK), murine monoclonal anti-Ki67, a nuclear cell proliferation-associated antigen (1:50, BD Pharmingen, Germany). Secondary antibodies (biotinylated goat anti-mouse and anti-rat) were obtained from Vector Laboratories. For double labeling secondary antibodies FITC-conjugated goat anti rabbit and Cy3-conjugated goat anti mouse (both from DIANOVA) were used. Furthermore, sections were stained after deparaffinization and rehydration with luxol fast blue (LFB)-periodic acid Schiff's.

Morphometric analysis

The extent of de- and remyelination was evaluated using a graded scoring system [16]. LFB stained and myelin protein (PLP, MBP, MOG) stained sections from 5 animals for each time point were scored in a double-blinded manner by three investigators (CT, SH, ML) and graded on a scale from 0 (complete myelination) to 3 (complete demyelination). For baseline, week 6 (complete demyelination) and week 7 (early remyelination) EM studies were additionally performed. A minimum of at least 300 axons per animal were analyzed. G-ratio (axon diameter divided by fibre diameter) and percentage of myelinated axons were measured [29].

The number of immunostained cells was determined in two to four standardized fields (for GFAP, MAC-3 and Nogo-A: 0.0625 mm^2, for NG2: 0.25 mm^2) in the corpus callosum using a Leica DMLB microscope.

Statistical analyses

As the data were not normally distributed (Kolmogorow-Smirnov test) the nonparametric Mann Whitney rank sum test was applied to evaluate differences

between IFN-β k/o mice and wt controls. Between the time points week 6 (end of demyelination) and week 7 (1 week of remyelination) we additionally performed a univariate analysis of variance to test for between-subjects effects. A p value < 0.05 was considered statistically significant.

Results

IFN-β k/o mice show normal myelin development

To ensure that IFN-β k/o mice show a normal myelination pattern during development, myelination and the presence and distribution of astrocytes and oligodendrocytes were investigated in the corpus callosum at several time points (1, 6, and 21 days of age and at 8 weeks) and compared to wt animals. NG2-positive cells were found in the corpus callosum as early as 1 day post partum in both animal groups. Numbers were highest early in the development and gradually decreased comparable in both animal groups (data not shown). IHC analysis of the myelin proteins PLP, MBP, MOG, and LFB myelin staining showed concordantly no myelin at the time points 1 and 6 days in wt animals as well as in IFN-β k/o mice. First signs of myelination were observed at 3 weeks of age. There were no differences in distribution and intensity of myelin proteins between IFN-β k/o mice and wt controls at this time point. Similarly, we could also not detect any differences in myelination patterns at 8 weeks of age. GFAP-positive cells were first found in the corpus callosum at an age of 3 weeks. Numbers and distribution revealed no differences between IFN-β k/o and wt mice. At week 8 of age, representing baseline levels for cuprizone feeding, again no differences in distribution and occurrence of GFAP-positive cells were observed between the two animal groups.

Taken together, IFN-β k/o mice showed the same myelination pattern during development as wt animals in the corpus callosum. Furthermore, no differences in distribution, occurrence, and quantity of GFAP- and NG2-positive cells were found between IFN-β k/o and wt mice during development. Therefore, conditions in IFN-β

k/o mice and wt animals were comparable at baseline levels (8 weeks of age) for the cuprizone model.

IFN-β k/o mice show only minor differences in demyelination in the cuprizone model

Extent of demyelination was evaluated by scoring of LFB staining and IHC for the myelin proteins PLP, MBP, and MOG at baseline and at week 3 and 6 during cuprizone feeding. All animals showed a decline in body weight, which was not significantly different between the two groups (data not shown). IFN-β k/o animals and wt animals showed no significant change in behaviour during the study. Demyelination occurred in all animals after 3 weeks of cuprizone feeding and was nearly complete at week 6. As compared to wt animals, IFN-β k/o mice showed less demyelination at week 3 as assessed by LFB scoring ($p=0.019$) and at week 6 as assessed by MOG IHC ($p=0.001$, see table 1 and figure 1). Scoring of the myelin proteins PLP and MBP did not show differences in demyelination between k/o and wt animals (table 1). EM analysis of baseline and week 6 confirmed extensive demyelination in both, k/o and wt mice at week 6 (G-ratio: wt baseline: 0.819 ± 0.0217; k/o baseline: 0.825 ± 0.0078; wt week 6: 0.92 ± 0.0138; k/o week 6: 0.928 ± 0.0409; percent myelinated axons: wt baseline: 85.8 ± 5.3%; k/o baseline: 87.3 ± 2.6%; wt week 6: 47.3 ± 3.4%; k/o week 6: 50.5 ± 10.4%). EM also confirmed that there was a minimal difference between k/o and wt mice at week 6 with k/o mice showing more percent myelinated axons than wt animals. However, this result was not statistically significant.

Microglial and astrocytic response to cuprizone-induced demyelination was diminished in IFN-β k/o mice

Astrocytic and microglial response was evaluated by quantifying GFAP or MAC-3-positive cells, respectively, within the corpus callosum. At baseline, neither IFN-β k/o mice nor wt mice showed detectable MAC-3 reactivity within the corpus callosum (figure 2a). During cuprizone feeding and toxic demyelination within the corpus callosum a remarkable increase of MAC-3 reactivity was observed with a maximum at week 3. Morphologically, MAC-3 positive cells resembled activated microglial cells and macrophages (figure 2b and c). Compared to wt animals, IFN-β k/o mice showed significantly less MAC-3 positive cells within the corpus callosum at week 3 ($p=0.025$, figure 2a). Microglial response was less pronounced at week 6 in both animal groups.

The number of GFAP-positive cells within the corpus callosum at baseline was not significantly different between wt animals and IFN-β k/o mice (figure 3a). During cuprizone induced demyelination the number of astrocytes within the corpus callosum increased and showed their maximum parallel to the maximum of demyelination at week 6 in both animal groups. Compared to wt mice, IFN-β k/o mice showed significantly reduced numbers of GFAP-positive cells at week 6 ($p=0.019$, figure 3).

The number of OPC significantly increased in IFN-β k/o mice during demyelination

The number of OPC within the corpus callosum and the subventricular zone (SVZ) was assessed by quantitative analysis of NG2 IHC. NG2-positive cells resembled morphologically OPC. At baseline the number of NG2-positive cells within the corpus callosum was not significantly different between wt animals and IFN-β k/o mice (figure 4a). During cuprizone induced demyelination, we observed an increase of

NG2-positive cells within the corpus callosum in both animal groups. In the wt animals NG2-positive cell infiltration within the corpus callosum reached its maximum at 3 weeks and showed a rapid decline to almost baseline levels at week 6. In contrast, in the IFN-β k/o mice NG2 cell numbers increased during the whole demyelination phase with a maximum at week 6. Compared to wt animals, we observed a significantly higher number of NG2-cells within the corpus callosum at week 6 ($p=0.046$, figure 4a).

OPC are found within the SVZ in the adult brain. Several studies support the hypothesis that after a demyelinating insult new OPC are generated in vivo in the SVZ and that these new OPC contribute to myelin repair [21,25,20]. Therefore, we also investigated NG2-positive cells in the SVZ. At baseline, wt animals and IFN-β k/o mice had comparable numbers of NG2-positive cells in the SVZ. During cuprizone feeding a gradual increase of NG2-positive cells within the SVZ was observed in IFN-β k/o mice with a maximum at week 6, but not in the wt animals ($p=0.011$, figure 4b-d).

Double labeling of NG2 with the proliferation marker Ki-67 was performed at time point week 6 to evaluate whether higher numbers of OPC in the IFN-β k/o were reflected in a higher proliferation rate (figure 5). The percentage of NG2-positive/Ki-67-positive cells out of the total of proliferating (Ki-67-positive) cells was quantified. In the wt animals 38.3 % (30-50 %) of all Ki-67-positive cells were OPCs whereas in the IFN-β k/o mice half of the proliferating cells were NG2-positive (54.7 %, 43.8-65 %). These data suggest that knockout mice showed a higher rate of proliferating OPCs at week 6 ($p=0.042$).

Oligodendrocytes are depleted during cuprizone-induced demyelination

Nogo-A was recently described as a reliable oligodendroglial marker [14] and quantification of immunohistochemistry for Nogo-A was therefore used to analyze the fate of oligodendrocytes during cuprizone-induced demyelination in wt and IFN-β k/o mice. At baseline a considerable amount of oligodendrocytes were found with no differences between the two groups (figure 6). After three weeks of cuprizone feeding oligodendrocytes were almost completely depleted from the corpus callosum in both animal groups. Interestingly, oligodendrocyte numbers recovered already during cuprizone feeding and reached higher numbers than baseline at week 6 with no differences between IFN-β k/o mice and control animals.

IFN-β k/o mice show a more rapid remyelination after cuprizone-induced demyelination

The extent of remyelination was evaluated by scoring of LFB stainings and IHC for the myelin proteins PLP, MBP, and MOG at three time points during remyelination: at week 7 which corresponded to 1 week of remyelination, at week 9 (= 3 weeks of remyelination) and week 12 (= 6 weeks of remyelination). Spontaneous remyelination occurred in all animals as soon as cuprizone was withdrawn from the food (see table 1 and figure 1). As compared to wt animals, IFN-β k/o mice showed a more rapid remyelination after one week of remyelination (week 7) (Mann Whitney rank sum test: LFB, $p=0.03$; PLP, $p=0.003$; MOG, $p=0.001$; univariate analysis of variance: LFB, $p=0.037$; PLP, $p<0.007$; MOG, $p<0.001$; table 1 and figure 1). Electron microscopy analysis at this time point confirmed that IFN-β k/o mice showed more myelinated axons than wt controls (IFN-β k/o: 63.8±4.5% of axons myelinated, wt: 54.5±3.2%, $p=0.044$, figure 7). The assessment of the G-ratio confirmed remyelination as compared to week 6, but did not show significant differences between the two animal groups.

After 6 weeks of remyelination (week 12) there was no difference between IFN-β k/o animals and controls observable anymore. However, compared to baseline remyelination was incomplete in all animals (table 1).

During remyelination NG2 cell numbers in the corpus callosum and the SVZ declined in both animal groups rapidly to roughly baseline levels and no longer showed differences between the two animal groups (figure 4a and b).

Numbers of Nogo-A-positive oligodendrocytes in the corpus callosum showed no differences between the two groups and remained higher than at baseline (figure 6).

The microglial response showed a gradual decline during the remyelination phase (figure 2a). At the end of the observation period (week 12) there were still some scattered MAC-3 positive cells within the corpus callosum in both animal groups. No differences between IFN-β k/o mice and wt were observed.

During remyelination astrocytic infiltration in the corpus callosum gradually diminished in both animal groups (figure 3). At week 12 numbers of GFAP-positive cells within the corpus callosum were still significantly higher compared to baseline numbers ($p<0.001$), but not different between IFN-β k/o and wt animals.

Cuprizone induced demyelination was not associated with axonal pathology

IHC for the non-phosphorylated neurofilament (SMI-32) served for the assessment of axonal pathology. Evaluation of SMI-32 stainings showed at none of the investigated time points signs of axonal pathology in both animal groups (data not shown).

Discussion

Here, we investigated whether the lack of endogenous IFN-β influences de- and remyelination in the cuprizone model. We favoured the cuprizone model for our investigations as it represents a toxin induced demyelination model and allows differentiating direct effects of IFN-β from immunomodulatory effects that are also known for IFN-β. IFN-β k/o mice showed only minor differences in cuprizone-induced demyelination as compared to wt controls. Demyelination was paralleled by a diminished microglial and astrocytic response in the IFN-β k/o mice as compared to wt controls. Recruitment and activation of microglial cells in demyelinated lesions is dependent on chemokines among other factors. IFN-β induces genes such as CCL4 and CCL5 in microglial cells, two chemokines, which play a role in recruitment and activation of microglia and macrophages [13]. Inflammatory mediators such as tumor necrosis factor-alpha (TNF-α), interleukin-1-beta (IL-1β), and nitric oxide (NO) were upregulated when microglial cells were treated with IFN-β in vitro [12]. A lack of IFN-β might therefore lead to less recruitment and activation of microglia cells and less inflammatory mediators during demyelination. However, since demyelination in the cuprizone model is not mediated by inflammatory mechanisms, we observed only minor differences between k/o and wt animals during demyelination.

In an inflammatory model of demyelination Njenga and colleagues reported that long term treatment with IFN-β of Theiler virus infected mice led to an aggravation of demyelination as compared to vehicle treated animals [22]. In contrast, Teige et al. showed that IFN-β k/o mice were more susceptible to experimental autoimmune encephalomyelitis (EAE) as compared to wt controls [30]. Furthermore, IFN-β k/o

mice developed a more severe and chronic disease with extensive inflammation and demyelination. They proposed that the effect of endogenous IFN-β is predominantly exerted in the effector phase of EAE with particularly extensive microglial activation and increase in effector functions of T cells. Clearly, mechanisms leading to demyelination are different in the cuprizone model as compared to EAE and most likely IFN-β exerts different functions in immune-mediated and toxic induced demyelination. However, microglial activation and modulation by IFN-β seem to play an important role. Mastronardi and colleagues reported that mice treated with IFN-β showed milder disease scores in an acute and chronic-relapsing EAE model as compared to wt controls [18]. The effect was accounted to a decreased astroglial response with no effect on leukocyte infiltration. Taken these data together, IFN-β affects the extent and dynamics of CNS demyelination in different animal models.

Withdrawal of cuprizone is followed reproducibly by a spontaneous remyelination of the corpus callosum within several weeks. In IFN-β k/o mice the extent of remyelination achieved after 6 weeks was comparable to wt animals. Interestingly, within the first week remyelination in IFN-β k/o mice was almost complete. Compared to wt animals remyelination in IFN-β k/o mice was therefore accelerated. This fast response was paralleled by the presence of threefold higher numbers of OPC within the corpus callosum and the SVZ at the beginning of the remyelination phase, but not by higher numbers of Nogo-A-positive oligodendrocytes. The increased numbers of NG2-positive cells in both the corpus callosum and the SVZ at peak of demyelination in IFN-β k/o mice suggests that there may be a more efficient recruitment or higher proliferation rate of OPC. Indeed, IFN-β k/o showed a higher number of proliferating NG2-positive cells at week 6.

We have previously shown that IFN-β significantly inhibits the differentiation of OPC in vitro when cultured in the presence of microglia and astrocytes [10]. In the in vivo setting however IFN-β mediated inhibition on OPC differentiation seems to be compensated as numbers of oligodendrocytes did not differ between k/o and wt animals. It was previously shown that migration of OPC was not altered by IFN-β treatment in vitro [9]. Various factors influence proliferation, migration and survival of OPC, among them, secreted factors by microglial cells and astrocytes [15]. For example, hyaluronan synthesized by astrocytes accumulates in demyelinated lesions and inhibits OPC maturation [1]. It is therefore feasible that the higher numbers of OPC in the corpus callosum and in the SVZ of IFN-β k/o mice could be explained by a less inhibitory environment due to a reduced microglial and astroglial response in the absence of IFN-β.

In summary, our data point to a modulatory function of IFN-β during de- and remyelination. In particular, IFN-β k/o mice showed an accelerated remyelination which was paralleled by an increased number of OPC at the end of the demyelination phase and the beginning of remyelination. Furthermore, less microglia and astrocyte responses were observed in IFN-β k/o mice. Taken together, the lack of IFN-β allows repair mechanisms to be implemented more rapidly, however, in the overall remyelination potential the lack of IFN-β is compensated.

Acknowledgements

The work was partially supported by the Deutsche Forschungsgemeinschaft (DFG, SFB 566, project A11).

Figure legends

Figure 1: Immunohistochemistry and quantitative analysis of MOG

Panels **a-c** show MOG immunohistochemistry of a coronal section of the corpus callosum of a representative control wt animal at baseline (**a**), 6 weeks of cuprizone feeding (**b**) and 1 week of remyelination (time point 7 weeks). Whereas panels **e** (time point 6 weeks) and **f** (time point 7 weeks) show MOG immunohistochemistry of IFN-β k/o animals. 6 Weeks of cuprizone feeding led to a complete demyelination of the corpus callosum in the wt animals as depicted in panel **b** with almost no MOG reactivity in the transversely traveling fibers of the corpus callosum at this time point. In comparison, MOG immunohistochemistry in IFN-β k/o mice still labeled scattered fibers in the corpus callosum indicating an incomplete demyelination. Withdrawal of cuprizone led to a spontaneous remyelination that could be observed as early as 1 week of withdrawal (time point 7 weeks) as shown in panels **c** (wt) and **f** (IFN-β k/o) by a reoccurrence of MOG-positive fibers. In comparison, IFN-β k/o mice show a more intense staining and more stained fibers indicating a more rapid remyelination. Bar in **a-c** and **e-f** represents 100 nm.

Panel **d**: MOG stained sections from 5 animals for each time point and animal group were scored using a graded scale from 0 (complete myelination) to 3 (complete demyelination). Depicted are mean values and bars for standard deviation. Open circles represent IFN-β k/o mice and filled circles wt controls. The remyelination phase is highlighted by changing background coloration. wks=weeks

Figure 2: Immunohistochemistry and quantitative analysis of MAC-3

Immunohistochemistry for MAC-3 was used to evaluate and quantify the microglial response. MAC-3 positive cells were counted in a standardized field within the corpus callosum in 5 animals at different time points and in both animal groups. Cell numbers are given in panel **a** as cells/mm^2 in mean values with bars for standard deviation. Open circles represent IFN-β k/o mice and filled circles wt controls. The remyelination phase is highlighted by changing background coloration. wks=weeks. The maximum of microglial infiltration was observed at 3 weeks in both animal groups. In comparison, IFN-β k/o mice showed less infiltrate (p=0.025). Panels **b** and **c** show representative immunohistochemical stainings of MAC-3 in a wt animal (**b**) and in a IFN-β k/o mouse (**c**) at week 3. Bars in **b** and **c** represent 10µm.

Figure 3: Immunohistochemistry and quantitative analysis of GFAP

Immunohistochemistry for GFAP was used to evaluate and quantify the astrocyticresponse. GFAP positive cells were counted in a standardized field within the corpus callosum in 5 animals at different time points and in both animal groups. Cell numbers are given in panel a as cells/mm^2 in mean values with bars for standard deviation. Open circles represent IFN-β k/o mice and filled circles wt controls. The remyelination phase is highlighted by changing background coloration. wks=weeks. The maximum of astrocyte infiltration was observed at 6 weeks in both animal groups. In comparison, IFN-β k/o mice showed less infiltrate (p=0.019). Panel **b** and **c** show representative immunohistochemical stainings of GFAP in a wt animal (**b**) and in a IFN-β k/o mouse (**c**) at week 6. Bars in **b** and **c** represent 10µm.

Figure 4: Immunohistochemistry and quantitative analysis of NG2

Immunohistochemistry for NG2 was used to evaluate and quantify OPC. NG2 positive cells were counted in a standardized field within the corpus callosum (**a**) and in the subventricular zone (SVZ, **b**) in 5 animals at different time points and in both animal groups. Cell numbers are given in panel **a** and **b** as cells/mm^2 in mean values with bars for standard deviation. Open circles represent IFN-β k/o mice and filled circles wt controls. The remyelination phase is highlighted by changing background coloration. wks=weeks. The OPC response showed different kinetics in wt and IFN-β k/o mice. In the wt animals we observed an increase of OPC numbers in the corpus callosum during early demyelination with a maximum at time point 3 weeks (**a**). In the SVZ OPC numbers didn't change much in wt animals (**b**). In contrast, IFN-β k/o mice showed a steady increase of OPC numbers during demyelination with a maximum at week 6 in both, the corpus callosum (**a**) and in the SVZ (**b**). Panel **c** and **d** show representative immunohistochemical stainings of NG2 of the SVZ in a wt animal (**c**) and in a IFN-β k/o mouse (**d**) at week 6. Bars in **c** and **d** represent 10µm.

Figure 5: Double immunohistochemistry for NG2 and the proliferation marker Ki-67

Double immunohistochemistry for NG2 and Ki-67 revealed proliferating OPC in the corpus callosum at time point week 6 in a IFN-β k/o animal.

Ki-67 is shown in red in **a**, NG2 is shown in green in **b**, DAPI nuclear counterstain is depicted in blue in **c**. **d** shows a merged figure of **a**-**c**. Bars represent 50 µm.

Figure 6: Immunohistochemistry and quantitative analysis of Nogo-A

Immunohistochemistry for Nogo-A was used to evaluate and quantify oligodendrocytes. Nogo-A positive cells were counted in a standardized field within

the corpus callosum in 5 animals at different time points and in both animal groups. Cell numbers are given in panel **a** as cells/mm^2 in mean values with bars for standard deviation. Open circles represent IFN-β k/o mice and filled circles wt controls. The remyelination phase is highlighted by changing background coloration. wks=weeks. During demyelination numbers of oligodendrocytes were almost completely depleted. Interestingly, oligodendrocytes already recovered during the demyelination phase. There were no differences between k/o and wt animals. Panel **b** shows a representative immunohistochemical staining of Nogo-A in a IFN-β k/o mouse at week 6. Bar in **b** represents 50µm.

Figure 7: Electronmicroscopy of the corpus callosum at week 7 (early remyelination)

EM analysis of the corpus callosum at week 7 (1 week of remyelination) confirmed more myelinated fibers in the IFN-β k/o mice (**b**) as compared to the wt mice (**a**).

Literature

1. Back SA, Tuohy TM, Chen H, Wallingford N, Craig A, Struve J, Luo NL, Banine F, Liu Y, Chang A, Trapp BD, Bebo BF, Jr., Rao MS, Sherman LS (2005) Hyaluronan accumulates in demyelinated lesions and inhibits oligodendrocyte progenitor maturation. Nat Med 11 :966-972

2. Baumann N, Pham-Dinh D (2001) Biology of oligodendrocyte and myelin in the mammalian central nervous system. Physiol Rev 81 :871-927

3. Bozzali M, Wrabetz L (2004) Axonal signals and oligodendrocyte differentiation. Neurochem Res 29 :979-988

4. Calabresi PA, Pelfrey CM, Tranquill LR, Maloni H, McFarland HF (1997) VLA-4 expression on peripheral blood lymphocytes is downregulated after treatment of multiple sclerosis with interferon beta. Neurology 49 :1111-1116

5. Calabresi PA, Tranquill LR, Dambrosia JM, Stone LA, Maloni H, Bash CN, Frank JA, McFarland HF (1997) Increases in soluble VCAM-1 correlate with a decrease in MRI lesions in multiple sclerosis treated with interferon beta-1b. Ann Neurol 41 :669-674

6. Chabot S, Williams G, Yong VW (1997) Microglial production of TNF-alpha is induced by activated T lymphocytes. Involvement of VLA-4 and inhibition by interferonbeta-1b. J Clin Invest 100 :604-612

7. Chan A, Seguin R, Magnus T, Papadimitriou C, Toyka KV, Antel JP, Gold R (2003) Phagocytosis of apoptotic inflammatory cells by microglia and its therapeutic implications: termination of CNS autoimmune inflammation and modulation by interferon-beta. Glia 43 :231-242

8. Erlandsson L, Blumenthal R, Eloranta ML, Engel H, Alm G, Weiss S, Leanderson T (1998) Interferon-beta is required for interferon-alpha production in mouse fibroblasts. Curr Biol 8 :223-226

9. Halfpenny CA, Scolding NJ (2003) Immune-modifying agents do not impair the survival, migration or proliferation of oligodendrocyte progenitors (CG-4) in vitro. J Neuroimmunol 139 :9-16

10. Heine S, Ebnet J, Maysami S, Stangel M (2006) Effects of interferon-beta on oligodendroglial cells. J Neuroimmunol 177 :173-180

11. Iarlori C, Reale M, Lugaresi A, De Luca G, Bonanni L, Di Iorio A, Feliciani C, Conti P, Gambi D (2000) RANTES production and expression is reduced in relapsing-remitting multiple sclerosis patients treated with interferon-beta-1b. J Neuroimmunol 107 :100-107

12. Kawanokuchi J, Mizuno T, Kato H, Mitsuma N, Suzumura A (2004) Effects of interferon-beta on microglial functions as inflammatory and antigen presenting cells in the central nervous system. Neuropharmacology 46 :734-742

13. Kim MO, Si Q, Zhou JN, Pestell RG, Brosnan CF, Locker J, Lee SC (2002) Interferon-beta activates multiple signaling cascades in primary human microglia. J Neurochem 81 :1361-1371

14. Kuhlmann T, Remington L, Maruschak B, Owens T, Brück W (2007) Nogo-A is a reliable oligodendroglial marker in adult human and mouse CNS and in demyelinated lesions. J Neuropathol Exp Neurol 66 :238-246

15. Li J, Baud O, Vartanian T, Volpe JJ, Rosenberg PA (2005) Peroxynitrite generated by inducible nitric oxide synthase and NADPH oxidase mediates microglial toxicity to oligodendrocytes. Proc Natl Acad Sci U S A 102 :9936-9941

16. Lindner M, Heine S, Haastert K, Garde N, Fokuhl J, Linsmeier F, Grothe C, Baumgärtner W, Stangel M (2007) Sequential myelin protein expression during remyelination reveals fast and efficient repair after central nervous system demyelination. Neuropathol Appl Neurobiol: in press

17. Lucchinetti C, Brück W, Parisi J, Scheithauer B, Rodriguez M, Lassmann H (1999) A quantitative analysis of oligodendrocytes in multiple sclerosis lesions. A study of 113 cases. Brain 122 (Pt 12) :2279-2295

18. Mastronardi FG, Min W, Wang H, Winer S, Dosch M, Boggs JM, Moscarello MA (2004) Attenuation of experimental autoimmune encephalomyelitis and nonimmune demyelination by IFN-beta plus vitamin B12: treatment to modify notch-1/sonic hedgehog balance. J Immunol 172 :6418-6426

19. Matsushima GK, Morell P (2001) The neurotoxicant, cuprizone, as a model to study demyelination and remyelination in the central nervous system. Brain Pathol 11 :107-116

20. Menn B, Garcia-Verdugo JM, Yaschine C, Gonzalez-Perez O, Rowitch D, Alvarez-Buylla A (2006) Origin of oligodendrocytes in the subventricular zone of the adult brain. J Neurosci 26 :7907-7918

21. Nait-Oumesmar B, Decker L, Lachapelle F, Avellana-Adalid V, Bachelin C, Van Evercooren AB (1999) Progenitor cells of the adult mouse subventricular zone proliferate, migrate and differentiate into oligodendrocytes after demyelination. Eur J Neurosci 11 :4357-4366

22. Njenga MK, Coenen MJ, DeCuir N, Yeh HY, Rodriguez M (2000) Short-term treatment with interferon-alpha/beta promotes remyelination, whereas long-term treatment aggravates demyelination in a murine model of multiple sclerosis. J Neurosci Res 59 :661-670

23. Okada K, Kuroda E, Yoshida Y, Yamashita U, Suzumura A, Tsuji S (2005) Effects of interferon-beta on the cytokine production of astrocytes. J Neuroimmunol 159 :48-54

24. Patrikios P, Stadelmann C, Kutzelnigg A, Rauschka H, Schmidbauer M, Laursen H, Sorensen PS, Bruck W, Lucchinetti C, Lassmann H (2006) Remyelination is extensive in a subset of multiple sclerosis patients. Brain 129 :3165-3172

25. Picard-Riera N, Decker L, Delarasse C, Goude K, Nait-Oumesmar B, Liblau R, Pham-Dinh D, Evercooren AB (2002) Experimental autoimmune encephalomyelitis mobilizes neural progenitors from the subventricular zone to undergo oligodendrogenesis in adult mice. Proc Natl Acad Sci U S A 99 :13211-13216

26. Rodriguez M (2003) A function of myelin is to protect axons from subsequent injury: implications for deficits in multiple sclerosis. Brain 126 :751-752

27. Sidman R, Angervine JB, Piece ET (1971) Atlas of the Mouse Brain and Spinal Cord. Commonwealth Fund Book Harvard University Press, Cambridge, MA

28. Smith KJ, Blakemore WF, McDonald WI (1981) The restoration of conduction by central remyelination. Brain 104 :383-404

29. Stidworthy MF, Genoud S, Suter U, Mantei N, Franklin RJ (2003) Quantifying the early stages of remyelination following cuprizone-induced demyelination. Brain Pathol 13 :329-339

30. Teige I, Treschow A, Teige A, Mattsson R, Navikas V, Leanderson T, Holmdahl R, Issazadeh-Navikas S (2003) IFN-beta gene deletion leads to augmented and chronic demyelinating experimental autoimmune encephalomyelitis. J Immunol 170 :4776-4784

31. Tuohy VK, Yu M, Yin L, Mathisen PM, Johnson JM, Kawczak JA (2000) Modulation of the IL-10/IL-12 cytokine circuit by interferon-beta inhibits the development of epitope spreading and disease progression in murine autoimmune encephalomyelitis. J Neuroimmunol 111 :55-63

32. Yong VW (2002) Differential mechanisms of action of interferon-beta and glatiramer aetate in MS. Neurology 59 :802-808

33. Zhao C, Fancy SP, Kotter MR, Li WW, Franklin RJ (2005) Mechanisms of CNS remyelination--the key to therapeutic advances. J Neurol Sci 233 :87-91

table

Click here to download table: Table 1 Trebst et al.doc

Table 1: Scoring of myelination

Weeks	LFB		PLP		MBP		MOG	
	wt	IFN-β k/o	wt	IFN-β k/o	wt	IFN-β k/o	wt	IFN-β k/o
baseline	0.25±0.45	0.50±0.67	0.08±0.29	0.08±0.29	0.17±0.39	0.38±0.48	0.25±0.45	0.21±0.40
3	**2.2±0.41**	**1.47±0.83**	1.5±0.46	1.47±0.70	1.93±0.92	1.57±0.90	1.27±0.53	1.33±0.70
6	2.87±0.35	2.6±0.83	2.87±0.35	2.67±0.49	2.13±0.64	2.33±0.75	**3.0±0**	**2.43±0.73**
7	**1.67±0.49**	**1.07±0.70**	**2.3±0.65**	**1.33±0.62**	0.75±0.64	0.93±0.80	**2.13±0.58**	**1.13±0.61**
9	0.6±0.51	0.73±0.46	1.67±0.49	2.1±0.64	0.77±0.75	1.23±0.82	2.03±0.64	1.63±0.61
12	1.07±0.59	0.93±0.59	1.47±1.19	1.27±0.84	1.08±0.79	0.83±0.65	1.5±0.71	1.27±0.56

The extent of de- and remyelination was evaluated using a graded scoring system. LFB, PLP, MBP and MOG stained sections from 5 animals for each timepoint were scored in a double-blinded manner by three investigators and graded on a scale from 0 (complete myelination) to 3 (complete demyelination). Shown are medians ± standard deviation. Significant differences are highlighted in bold letters. Remyelination phase is emphasized by a gray background. wt= wildtype control.

figure 1

Click here to download high resolution image

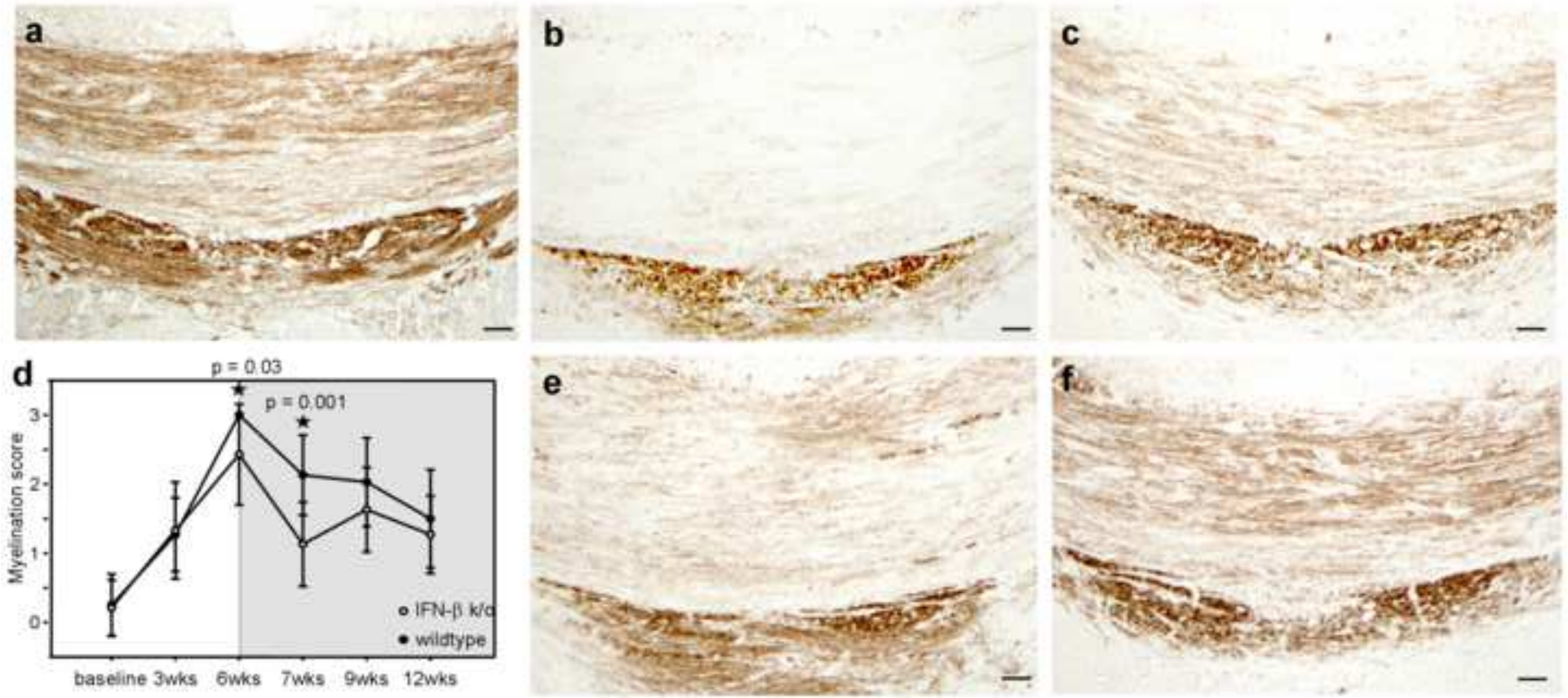

figure 2

Click here to download high resolution image

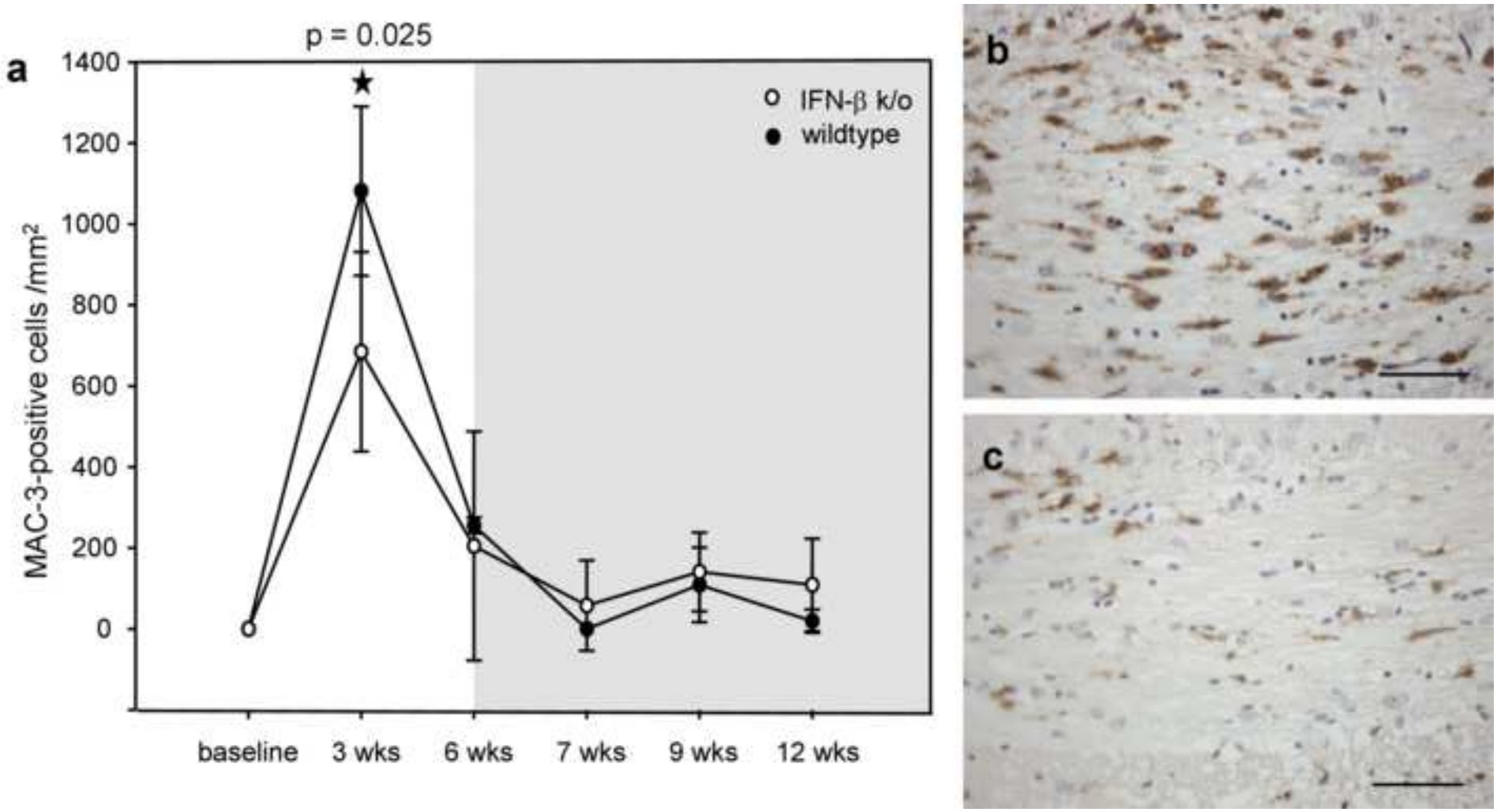

figure 3

Click here to download high resolution image

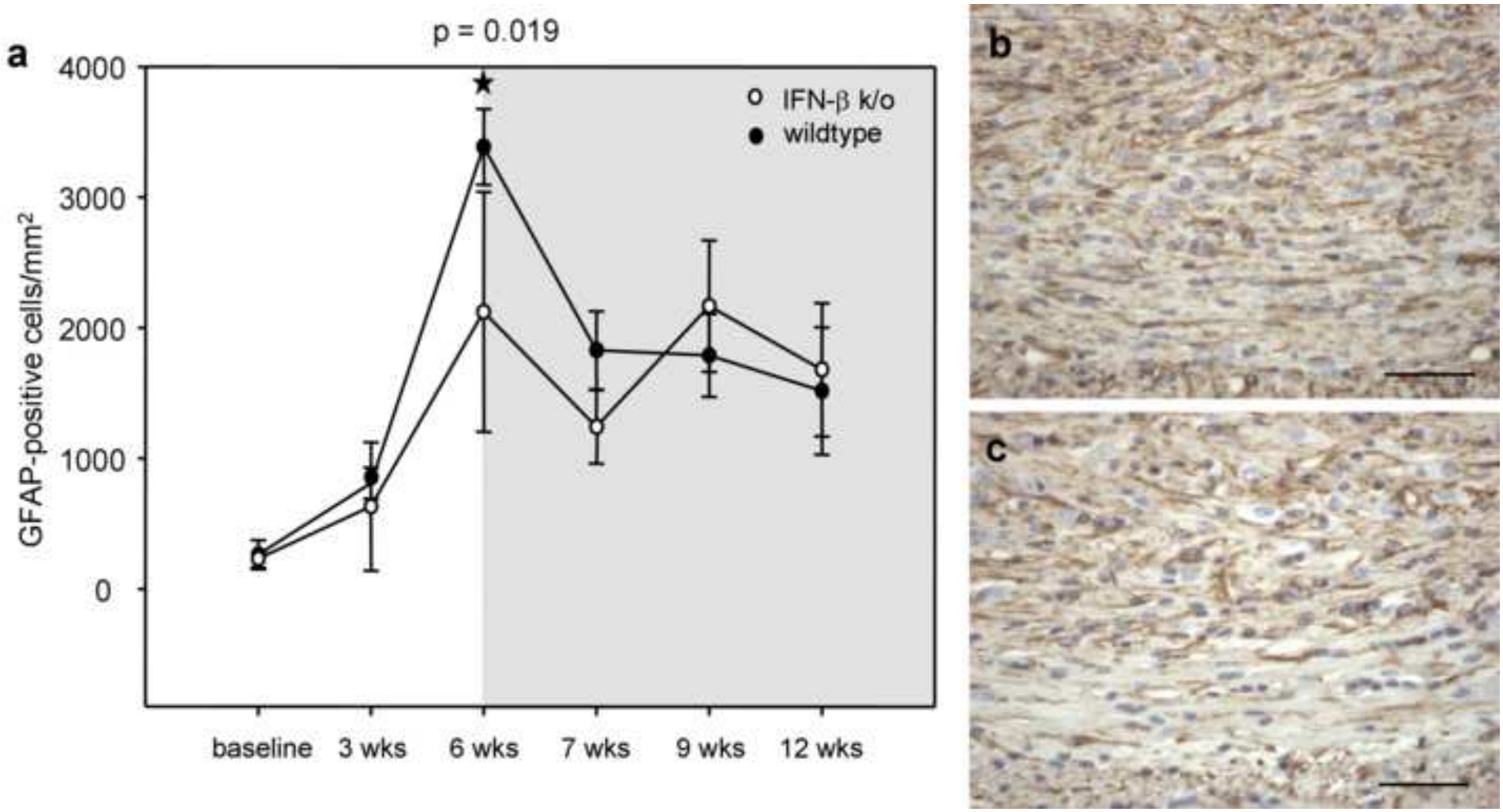

figure 4

Click here to download high resolution image

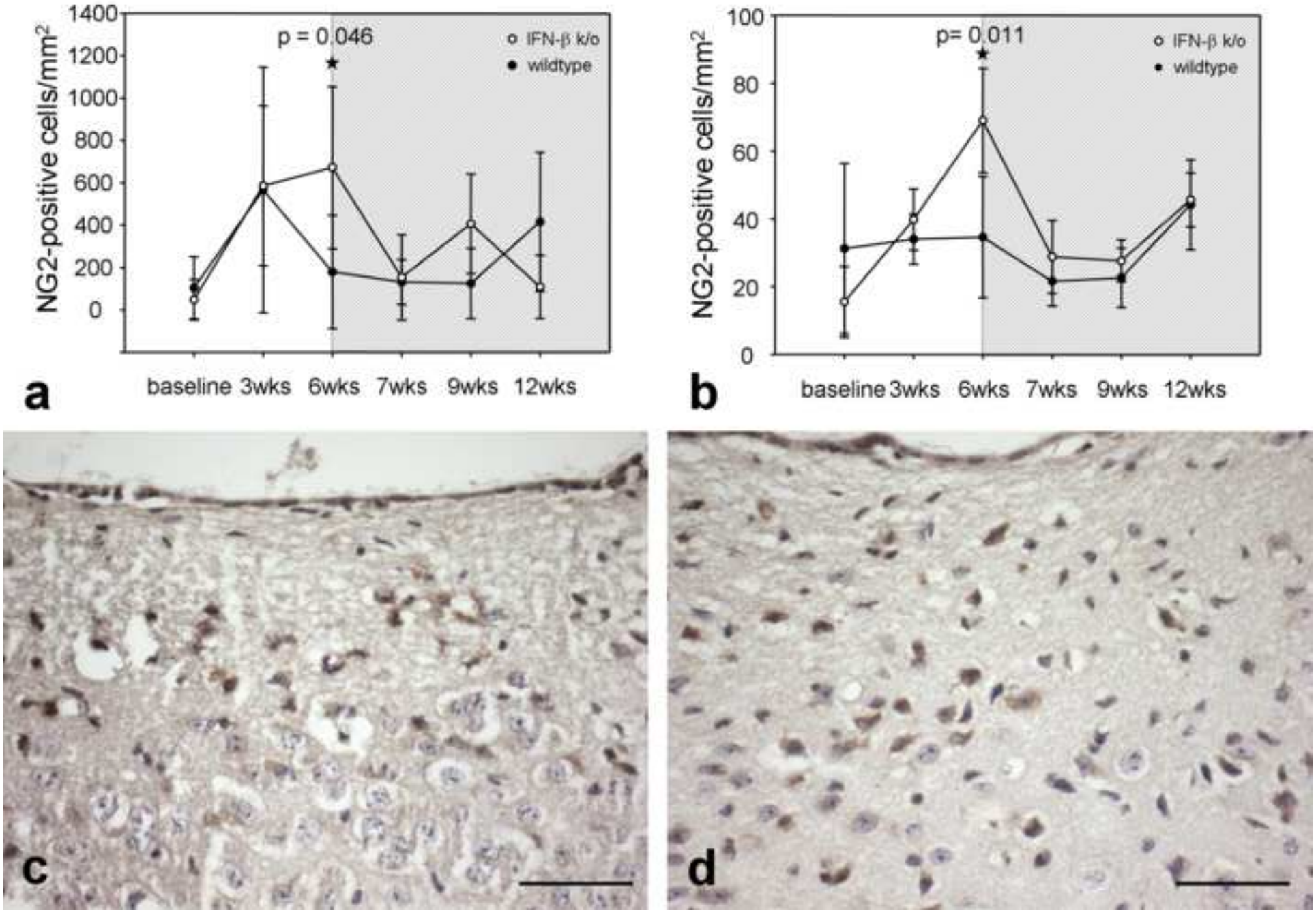

figure 5
Click here to download high resolution image

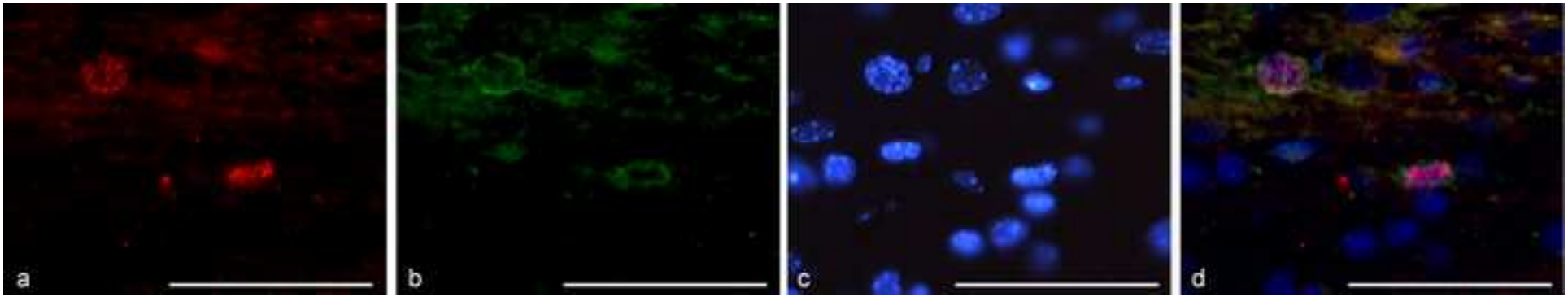

figure 6
Click here to download high resolution image

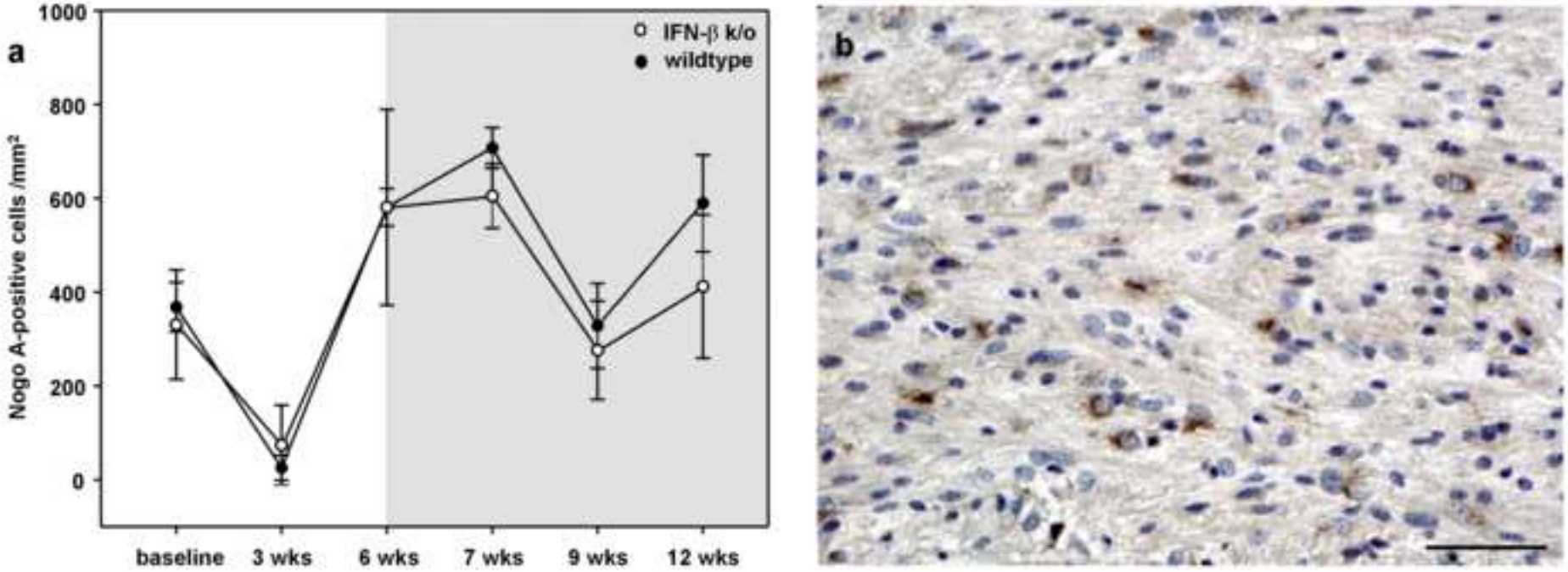

figure 7

Click here to download high resolution image